Transcription Factor ELF1 Activates MEIS1 Transcription and Then Regulates the GFI1/FBW7 Axis to Promote the Development of Glioma

Meixiong Cheng,[1] Yi Zeng,[2] Tian Zhang,[1] Min Xu,[2] Zhili Li,[1] and Yaqiu Wu[2]

[1]Department of Neurosurgery, Sichuan Provincial People's Hospital, School of Medicine, University of Electronic Science and Technology of China, Chengdu 610072, P.R. China; [2]Department of Neurosurgery Critical Care Medicine, Sichuan Provincial People's Hospital, School of Medicine, University of Electronic Science and Technology of China, Chengdu 610072, P.R. China

Glioma is the most common malignancy in the central nervous system with no immediate prospect of a cure. Comprehensive understanding on the pathogenesis of the disorder contributes to a better outcome. Herein, we aimed to investigate whether transcription factors erythroblast transformation-specific (ETS) transcription factor (ELF1), myeloid ecotropic viral integration site 1 (MEIS1), and growth factor independence 1 (GFI1)/F-box/WD repeat-containing protein 7 (FBW7) mediate progression of glioma. ELF1, MEIS1, and GFI1 were upregulated in glioma cells and tissues, as ELF1 was correlated with poor prognosis. Bioinformatics analysis identified the binding between ELF1 and MEIS1 as well as between GFI1 and FBW7, confirmed by chromatin immunoprecipitation (ChIP) experiments. Functional experiment indicated that silencing of ELT1 decreased MEIS1 expression and that overexpression of MEIS1 increased GFI1 expression by activating GFI1 enhancer but decreased FBW7 expression. Importantly, silencing of ELF1 decreased the capacities of proliferation, migration, and invasion of glioma cells whereas it increased apoptosis, supported by increased capase-3 and decreased matrix metalloproteinase-9 (MMP-9) and proliferating cell nuclear antigen (PCNA) expression. Moreover, an *in vivo* experiment confirmed the inhibitory role of silenced ELF1 in tumor growth, with a decreased level of MEIS1 and GFI1. Taken together, our study elucidated a potential mechanism that ELF1 promoted cell progression by increasing GFI1 and METS1 as well as decreasing FBW7 expression in glioma.

INTRODUCTION

Malignant gliomas are among the most common primary brain tumors in adults.[1] Due to the infiltrative nature of this disease and the localization close to eloquent brain areas, surgical resection fails to cure the disease. Patients diagnosed with a malignant glioma such as glioblastoma have to undergo a fierce clinical course with a survival time of less than 2 years for most patients.[2,3] Based on advances in the molecular characterization of these tumors, disease-associated targets, including epidermal growth factor receptor (EGFR) or vascular EGFR (VEGFR), were identified, which led to the development of new approaches using traditional routes of drug

development.[4–6] According to the World Health Organization (WHO) classification of tumors of the central nervous system, gliomas can be categorized into four grades (grades I–IV), among which grade IV is also called glioblastoma or glioblastoma multiforme (GBM).[7] Moreover, a gene expression-based molecular classification of glioblastoma has been presented, including proneural, neural, classical, and mesenchymal subtypes.[8] Despite the identification of these different subtypes, no effective targeted therapy for gliomas has been developed in recent decades to improve outcomes. Unfortunately, these strategies failed so far, because the complexity of the disease was underestimated and important factors such as the capability of therapeutics to pass the blood-brain barrier or to penetrate the tumor tissue were not sufficiently considered. This perspective is substantiated by the fact that areas of variant morphology exhibit significant differences in gene expression subtype within a single tumor yet harbor a large number of identical genetic alterations.[9]

Erythroblast transformation-specific (ETS) family transcription factors play important roles in prostate tumorigenesis, with some acting as oncogenes and others as tumor suppressors. ETS factors compete for binding at some *cis*-regulatory sequences. Therefore, changes in expression of ETS family members during tumorigenesis can have complex, multimodal effects. Recent research showed that ETS transcription factor 1 (ELF1) could serve as a possible factor for tumor progression.[10] Genome-wide mapping in cell lines indicated that ELF1 has two distinct tumor suppressive roles mediated by distinct *cis*-regulatory sequences. ELF1 and ELF2, closely related transcription factors to ELF4, also exerted a proliferative effect in various cancer cell

lines.[11] Furthermore, knockdown of ELF1 increased docetaxel resistance, indicating that the genomic deletions found in metastatic prostate tumors may promote therapeutic resistance through loss of c1 in glioma and can reduce its ability to recruit the transcription factor myeloid ecotropic viral integration site 1 (MEIS1), and further impair the activation ability of MEIS1 to growth factor independence 1 (GFI1) enhancer, resulting in suppression of proliferation, migration, and invasion and induction of cell apoptosis in glioma cells.[12] MEIS1, a transcription factor, exerts important functions in cell fate determination during development and cell proliferation.[13] GFI1 is located within chromosome 1p22 in the human genome, and as a zinc finger protein, GFI1 mainly functions as a transcriptional repressor by direct or functional interaction with other co-factors.[14] The tumor suppressive mechanisms of these normally expressed ETS factors and their interplay with oncogenic ETS factors are not well understood.

In our study, we aimed to investigate the mechanism underlying ELF1 mediating the progression of glioma. Our results revealed that interference of ELF1 in glioma reduced its ability to recruit the transcription factor MEIS1 and further impaired the activation ability of MEIS1 to GFI1 enhancer in glioma cells. Additionally, an animal model was also established to detect the impact of ELF1/MEIS1/GFI1 on tumor growth.

RESULTS

ELF1 Is Highly Expressed in Glioma Tissues and Correlates with WHO Grading and KPS Score of Patients

Datasets GEO: GSE12657, GSE35493, GSE104291, and GSE50161 were analyzed by R language, and we found 1,507, 4,173, 2,784, and 4,554 differentially expressed genes, respectively. We found that there were 578 genes expressed in these four datasets through coexpression analyzing using the RobustRankAggreg pack (Figure 1A). Eight key transcription factors were obtained from hTFtarget and Cistrome, including BCL11A, EZH2, FOXM1, HDAC1, ELF1, STAT4, CBX3, and VEZF1 (Figure 1B), among which ELF1 has been implicated as being associated with glioma.[15] The expression data from datasets GEO: GSE35493, GSE35493, GSE104291, and GSE50161 were presented in a boxplot where ELF1 was indicated as highly expressed in glioma, while Gene Expression Profiling Interactive Analysis (GEPIA) analysis of GBM data from GTEx dataset also identified the high expression of ELF1 (Figure 1C).

In order to determine whether ELF1 was involved in the occurrence and development of glioma, the expression of ELF1 in brain tissues of glioma patients (n = 60) and normal brain tissues (n = 24) was detected by qRT-PCR. Compared with the normal group, the expression of ELF1 in glioma tissues was significantly increased (Figure 1D). The expression of ELF1 increased with the increase of the WHO grade of glioma (p < 0.05) (Figure 1E). In addition, we analyzed the ELF1 expression and the link between the patient clinical pathological features. According to the ELF1 average expression in gliomas (1.695), it was divided into a high- and low-expression group. The results showed that the expression of ELF1 had an obvious correlation with the WHO classification and Karnofsky performance status

(KPS) scores in patients; however, there was no significant correlation between expression of ELF1 and patient's age, sex, tumor size, and tumor recurrence (Table 1). After Kaplan-Meier analysis, the log-rank test of survival data showed that expression of ELF1 was negatively correlated with survival time and prognosis of patients (Figure 1F).

Silencing ELF1 Inhibits the Proliferation, Migration, and Invasion of Glioma Cells and Promotes Cell Apoptosis

In view of the significant upregulation of ELF1 in glioma tissues, in order to determine how it affected the proliferation, migration, and invasion abilities of glioma cells, we performed functional experiments on glioma cells. We constructed small interfering RNA (siRNA) specific to ELF1 (si-ELF1-1, si-ELF1-2, si-ELF1-3), and si-ELF1 exhibited the most significant interference on ELF1 expression, according to the results from qRT-PCR (Figure S4A). After transfection with si-ELF1, the expression of ELF1 was significantly decreased in glioma cells A172, U251, and T98G according to results of qRT-PCR and western blot analysis (Figure 2A; Figure S1A). From the results of a Cell Counting Kit-8 (CCK-8) assay, transwell assay, and annexin V/propidium iodide (PI) dual staining, glioma cell abilities of proliferation, migration, and invasion were significantly inhibited and cell apoptosis was induced after interference of ELF1 (Figures 2B–2E; Figures S1B–S1E). Proliferation-related factor proliferating cell nuclear antigen (PCNA), invasion-related factor matrix metalloproteinase-9 (MMP-9), and apoptosis-related factor cleaved caspase-3 expression was detected by western blot analysis, and results showed that compared with the si-negative control (NC) group, expressions of PCNA and MMP-9 in the si-ELF1 group were significantly decreased, while expressions of cleaved caspase-3 were significantly increased (Figure 2F; Figure S1F).

Transcription Factor ELF1 Binds to the MEIS1 Promoter to Promote Its Transcription and Promote the Development of Glioma

In the above studies, we have identified that ELF1 was highly expressed in glioma tissues and can significantly inhibit the proliferation, migration, and invasion of glioma cells after specific interference treatment. Then, we continued our review of relevant literature and found that ELF1, a transcription factor, can be combined into MEIS1 promoter regions, thus affecting the transcription.[16] The normalized data of ELF1 and MEIS1 of 84 samples from datasets GEO: GSE12657, GSE35493, GSE104291, and GSE50161 identified a positive correlation between ELF1 and MEIS1 (Figure 3A). GEPIA analysis confirmed the positive correlation upon analysis of GBM data from The Cancer Genome Atlas (TCGA) dataset (Figure 3B). The analysis of the four datasets also revealed that MEIS1 was significant highly expressed in glioma tissues in the GEO: GSE35493 and GSE35492 datasets, while it was highly expressed in GEO: GSE104291 and GSE50161, but not significantly (p > 0.05) (Figure 3C). Based on this evidence, we hypothesized that ELF1 may affect glioma development by promoting the transcription of MEIS1. We initially detected MEIS1 expression in glioma tissues through the qRT-PCR and western blot analysis and identified the elevated expression of MEIS1 in glioma tissues relative to normal brain tissues
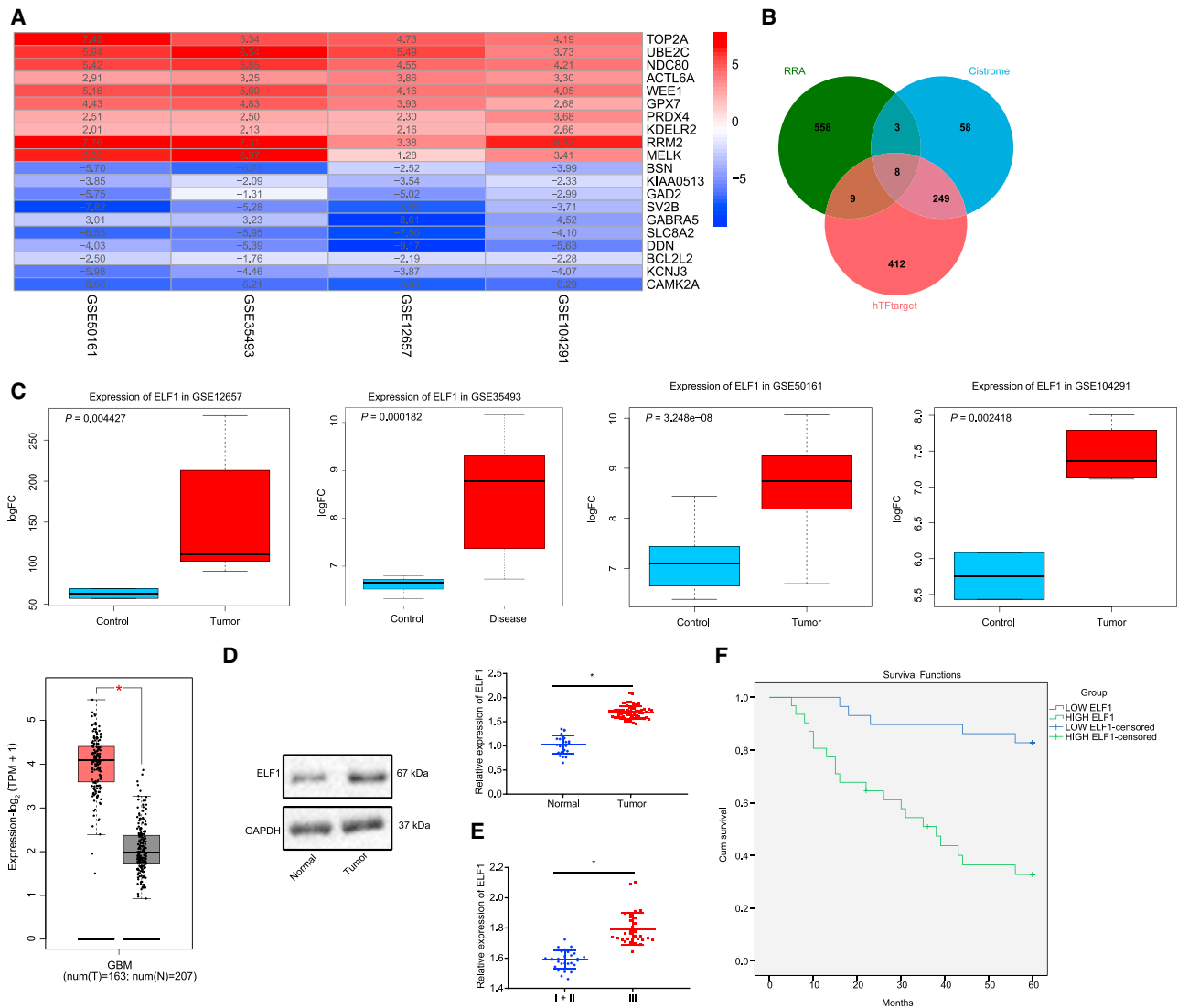
Figure 1. ELF1 Is Involved in the Development of Glioma

(A) Heatmap of differentially expressed genes screened from GEO: GSE50161, GSE35493, GSE12657, and GSE104291 datasets. (B) Venn diagram of the intersection of co-expression genes, transcription factors of the hTF target, and transcription factors of Cistrome through RobustRankAggreg. RRA refers to co-expression genes in four datasets through analysis of RobustRankAggreg. (C) Boxplot of ELF1 expression from the GEO: GSE12657, GSE35493, GSE50161, and GSE104291 datasets, as well as GBM data from TCGA dataset and GTEx through GEPIA analysis. (D) qRT-PCR analysis of ELF1 expression in clinical glioma tissues (n = 60) and normal brain tissues (n = 24). (E) Correlation of ELF1 expression and WHO grading in glioma patients. (F) Kaplan-Meier method to analyze the relationship between ELF1 expression and survival time of patients. The above measurement data are expressed as mean ± standard deviation. *p < 0.05 compared with the normal brain tissues or cases of I + II grade. An unpaired t test was used between the two groups.

(Figure 3D). The binding site between ELF1 and MEIS1 promoter obtained by the JASPAR dataset (Figure 3E; Table S1) was detected by a chromatin immunoprecipitation (ChIP) experiment. We applied magnetic protein A beads to precipitation and found that compared with the immunoglobulin G (IgG) group, the promoter DNA of binding MEIS1 in the ELF1 group was significantly increased (Figure 3F; Figure S2A). When si-ELF1 plasmids were transfected into glioma cells, mRNA and protein expressions of MEIS1 were significantly decreased (Figure 3G; Figure S2B).

Furthermore, to determine whether ELF1 was involved in the development of glioma through affecting the transcription of MEIS1, we transfected si-NC + overexpression (oe)-NC, si-ELF1+ oe-NC, and si-ELF1 + oe-MEIS1 into glioma cells A172, U251, and T98G, followed by transwell and CCK-8 assays, as well as annexin V/PI staining. It was clear that treatment with si-ELF1 + oe-NC decreased cell proliferation, migration, and invasion ability, whereas it increased apoptosis, in comparison with that of the control group. Based on si-ELF1, addition of oe-MEIS1 reversed the effect of ELF1

Table 1. The Relationship between ELF1 Expression and the Clinicopathological Characteristics of Glioma Patients

| Index | No. | ELF1 Expression | | p Values |
		Low Expression (n = 29)	High Expression (n = 31)	
Sex				
Male	38	20	18	0.431
Female	22	9	13	
Age (Years)				
≥63	35	16	19	0.794
<63	25	13	12	
Tumor Diameter (mm)				
≥5	33	15	18	0.796
<5	27	14	13	
TNM				
I~II	29	28	1	< 0.001
III~IV	31	1	30	
KPS				
≥70	35	27	8	< 0.001
<70	25	2	23	
Relapse				
Yes	37	14	23	0.062
No	23	15	8	
TNM, tumor-node-metastasis.				

interference on glioma cells, promoting the growth, migration, and invasion of glioma cells, and reducing cell apoptosis (Figures 3H–3K; Figures S2C–S2F).

Western blot analysis was then conducted to analyze proliferation factor PCNA, invasion-related protein MMP-9, and apoptosis key factor cleaved caspase-3 upon treatments. The expression of PCNA and MMP-9 in the si-ELF1 + oe-NC group was decreased and the expression of cleaved caspase-3 was increased. Similarly, overexpression of MEIS1 increased the expression of PCNA and MMP-9, and decreased cleaved caspase-3, restoring the expression of these key factors (Figure 3L; Figure S2G). These results suggested that the transcription factor ELF1 may be involved in glioma development by enhancing MEIS1 transcription in glioma.

MEIS1 Promotes Glioma Development by Regulating the Activity of the GFI1 Promoter

Multi Experiment Matrix (MEM) analysis, a visualization tool gathering publicly available gene expression data and ranking genes by their similarity, in the current study pointed to a co-expression relationship between MEIS1 and GFI1 (Figure 4A). To confirm this relationship in tissues, we then detected GFI1 expression in the glioma and normal control tissues by qRT-PCR and western blot analysis, and found that expression of GFI1 in glioma tissues was higher (Figure 4B). When glioma cells were transfected with overexpression of MEIS1, as demonstrated by western blot analysis, GFI1 expression

in cells was increased (Figure 4C; Figure S3A). Then, the ChIP experiment was used to verify the relationship between MEIS1 and GFI1. Overexpression of MEIS1 in A172, U251, and T98G cells led to the enrichment of H3K4me1, H3K27ac, and MEIS1 in the GFI1 promoter and enhancer region with similar results observed in the three cell lines. These results indicated that MEIS1 promoted the expression of GFI1 by activating the enhancer of GFI1 (Figures 4D and 4E; Figures S3B and S3C).

To further explore the impact between MEIS1 and GFI1 on glial development, we treated U251 cells with overexpressed MEIS1 or interfered GFI1 simultaneously, followed by a CCK-8 assay, transwell assay, and flow cytometry. Compared with the oe-NC+ si-NC group, cell proliferation, migration, and invasion were increased but the apoptosis rate was decreased in the oe-MEIS1 + si-NC group. The interference plasmids of GFI1 (si-GFI1-1, si-GFI1-2, si-GFI1-3) were established and si-GFI1-1 with greatest efficiency of interference was selected to transfect to oe-MEIS1-treated cells (Figure S4B). However, oe-MEIS1 + si-GFI1 reversed the effect of overexpressing MEIS1 on cell progression (Figures 3D–3G and 4F–4I). These results were supported by following the detection of MMP-9, cleaved caspase-3, and PCNA in the cells upon treatment. As displayed in Figure 4J and Figure S3H, interference with GFI1 could reverse the effect of overexpression of MEIS1 on all related proteins, inhibiting the expression of PCNA and MMP-9, and promoting the expression of cleaved caspase-3.

In the occurrence of cervical cancer, as reported, GFI1 can inhibit the expression of F-box/WD repeat-containing protein 7 (FBW7) through its correlation with FBW7.[17] Since the GEO: GSE12657 dataset does not include the expression data for FBW7 (named FBXW7 in NCBI), we only normalized the data concerning FBW7 from the other three datasets to assess the correlation between GFI1 and FBW7. We found that there was a negative correlation between GFI1 and FBW7 (Figure 4K). Analysis from the datasets GEO: GSE35493, GSE104291, and GSE35493 indicated poorly expressed expression of FBW7 in glioma, consistent with the results from TCGA and GTEx datasets analyzed by GEPIA (Figure 4L). GFI1 and FBW7 had a significantly co-expressed relationship, as evidenced by MEM analysis (Figure 4M). In addition, we continued to detect the expression of FBW7 in glioma cells by western blot analysis after transfection with MEIS1 or GFI1. As shown in Figure 4N and Figure S3I, compared with the oe-NC + si-NC group, FBW7 expression was significantly lower in the oe-MEIS1 + si-NC group, but additional treatment with si-GFI1 hardly altered expression of FBW7. This evidence elucidated a mechanism that MEIS1 inhibited FBW7 expression through mediating the activity of GFI1 and thereby promotes proliferation, migration, and invasion and inhibits apoptosis of glioma cells.

Interference with ELF1 Can Inhibit Glioma Progression *In Vivo* by the MEIS1/GFI1/FBW7 Axis

To confirm the *in vivo* anti-tumor effect of ELF1, we developed a mouse model. First, we silenced ELF1 expression in U251 cells and
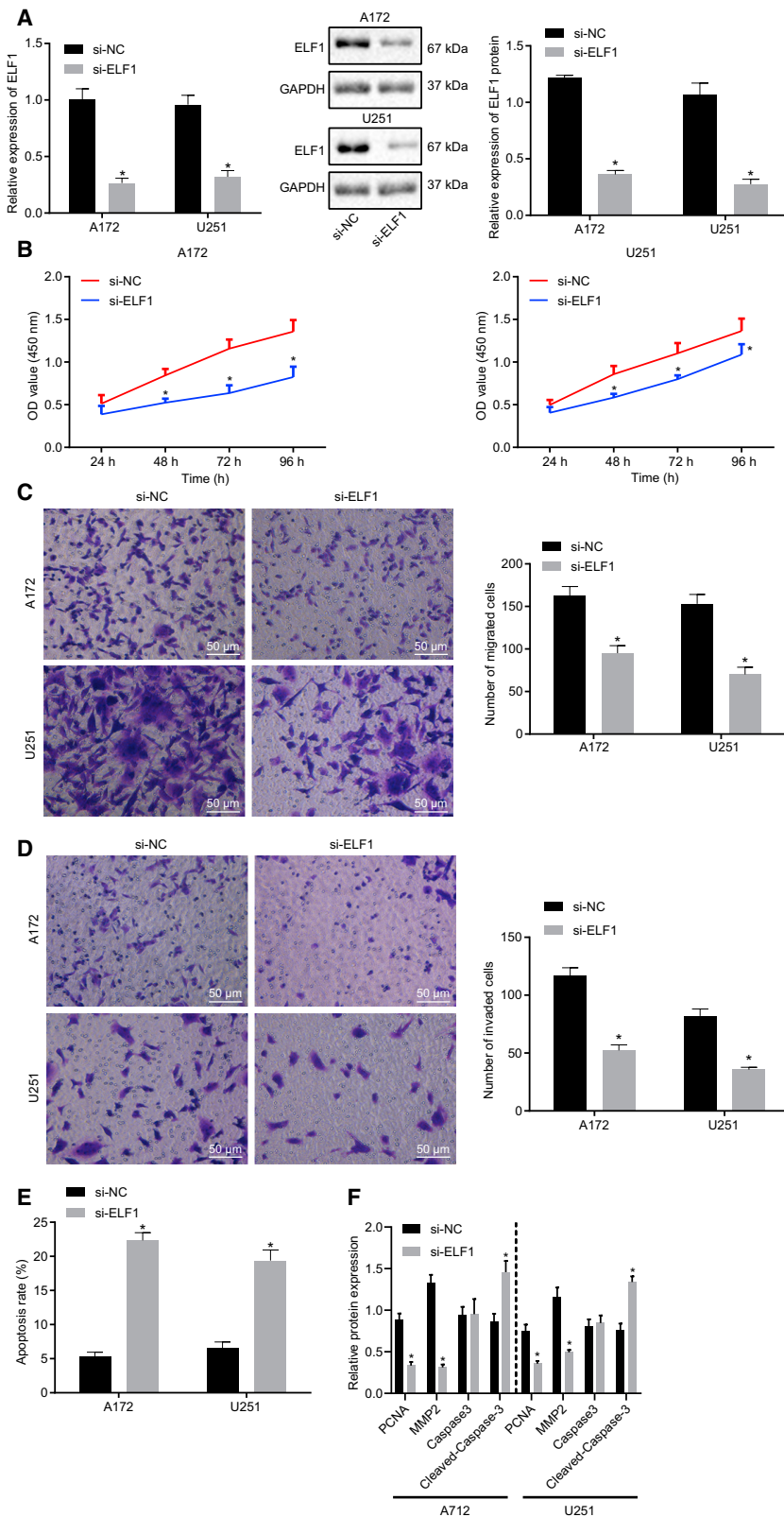
Figure 2. Silencing ELF1 Inhibits Proliferation, Migration, and Invasion and Promotes Apoptosis of A172 and U251 Glioma Cells

(A) Expression of ELF1 in A172 and U251 glioma cells upon si-NC or si-ELF1 was tested by qRT-PCR and western blot analysis. (B) CCK-8 assay of proliferation of A172 and U251 cells upon treatment with si-NC or si-ELF1. (C) Transwell assay of migration of A172 and U251 cells upon treatment with si-NC or si-ELF1 (original magnification, ×200). (D) Transwell assay of migration of A172 and U251 cells upon treatment with si-NC or si-ELF1 (original magnification, ×200). (E) Apoptosis rate of A172 and U251 cells was determined by annexin V/PI flow cytometry. (F) Western blot analysis was used to detect the expression of proliferation-related factor PCNA, invasion-related factor MMP-9, and apoptosis-related factor cleaved caspase-3 of A172 and U251 cells upon treatment with si-NC or si-ELF1. The above values are all measurement data, expressed as mean ± standard deviation. *$p < 0.05$ compared with the si-NC group. An unpaired t test was used between the two groups, and the data of each group at different time points were compared. The cell experiment was repeated three times.
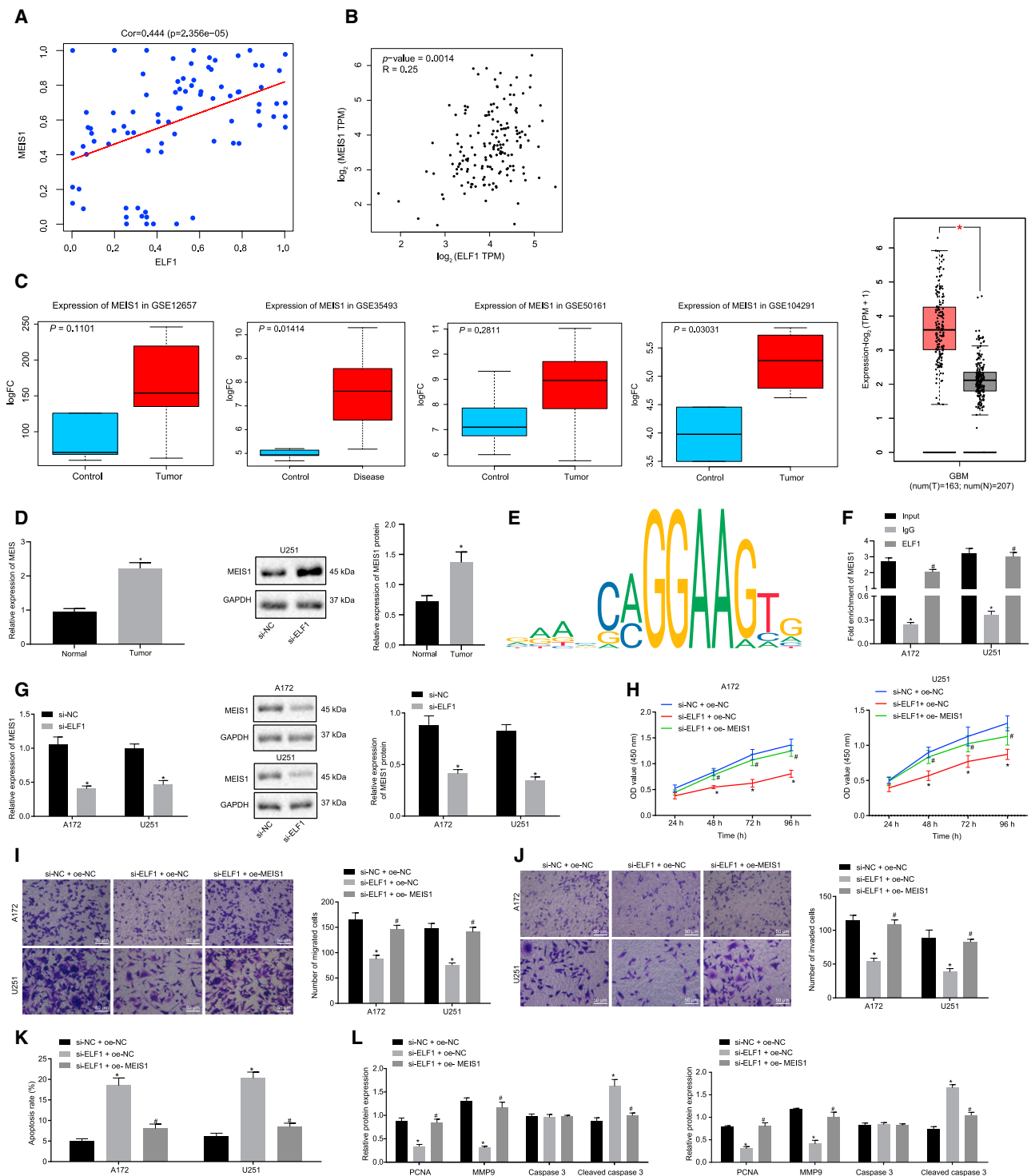
Figure 3. ELF1 Binds to the MEIS1 Promoter to Promote the Expression of MEIS1 to Participate in the Development of Glioma

(A) Normalized expression correlation diagram of ELF1 and MEIS1 drawn from GEO: GSE50161, GSE35493, GSE12657, and GSE104291 datasets. (B) Expression correlation diagram of ELF1 and MEIS1 through GEPIA analysis of GBM data from TCGA dataset. (C) Boxplot of MEIS1 expression from dataset GEO: GSE12657, GSE35493, GSE50161, and GSE104291, as well as GBM data from TCGA dataset and GTEx through GEPIA analysis. *p < 0.01. (D) qRT-PCR analysis of MEIS1 expression in clinical glioma tissues (n = 60) and normal brain tissues (n = 24). (E) Binding site of ELF1 and METS1 promoter through the JASPAR dataset. (F) ChIP experiment of METS1

(legend continued on next page)

transplanted the cells into the nude mice. Every week, we checked the weight and volume of the tumors. The results showed that the weight and volume of tumor in mice treated with sh-ELF1 were lower than those in the control group (Figures 5A–5C). In addition, western blot analysis showed that sh-ELF1 treatment significantly reduced the expression of ELF1, MEIS1, and GFI1, accompanied with elevated expression of FBW7 (Figure 5D). These results indicated that interference with ELF1 could inhibit MEIS1/GFI1, thereby promoting expression of FBW7 and retarding tumor growth *in vivo*.

DISCUSSION

Gliomas comprise the most common type of primary malignant brain tumor, and except for pilocytic astrocytoma and subependymal giant cell astrocytoma, nearly all are characterized by a high recurrence rate, high mortality, and short survival times. Only 5.5% of patients typically survive 5 years after diagnosis, and the median overall survival is still dismal at approximately 14.5–16.6 months, even with multimodal therapy comprised of surgery, radiotherapy, and chemotherapy.[8] In the present study, we demonstrated that interference of ELF1 in glioma can reduce its ability to recruit the transcription factor MEIS1 and further impair the activation ability of MEIS1 to GFI1 enhancer, resulting in the suppression of proliferation, migration, and invasion and induction of cell apoptosis in glioma cells.

ELF1 was identified as a potential downstream target of the DNA damage response pathway, and following ionizing radiation, U2OS cells with a siRNA against ELF1 were more likely to escape cell cycle arrest by bypassing the G_2-M checkpoint.[18–20] For the purpose of determining whether ELF1 was involved in the occurrence and development of glioma, we measured the expression of ELF1 in brain tissues of glioma patients and found that ELF1 is highly expressed in glioma tissues and closely correlates with WHO grading and the KPS score of patients. Therefore, we hypothesized that ELF1 might serve as a factor of tumor promotion. In order to verify our hypothesis, we silenced the ELF1 in A172, U251, and T98G cell lines and found that the proliferation activity of cells was significantly decreased. Additionally, silencing of ELF1 dramatically triggered apoptosis in A172, U251, and T98G cell lines. Furthermore, activities of migration and invasion of glioma cells were distinctly impaired by silencing of ELF1. The proliferation-related factor PCNA and invasion-related factor MMP-9 were downregulated, while apoptosis-related factor cleaved caspase-3 was upregulated after interference of ELF1 in glioma cells. The above results suggested that silencing ELF1 inhibits the proliferation, migration, and invasion and promotes cell apoptosis of glioma cells.

MEIS1 is a transcription factor that regulates important functions in cell fate determination during development and cell proliferation.[13] MEIS1 has a key role in the regulation of the stemness state of stem cells and the transcription adjustment of self-renewal genes, as well as involved genes in cell development and differentiation, playing an oncogenic role in several tumors.[21] It has been reported that ELF1 can act as an important positive transcriptional regulator of the Hox cofactor MEIS1.[16] Therefore, we hypothesized that ELF1 may affect glioma development by regulating the transcription of MEIS1. Based on the results from qRT-PCR, the expression of MEIS1 in glioma tissues was significantly upregulated in comparison to normal tissues. In addition, overexpression of MEIS1 reversed the effect of ELF1 interference on promoting the growth, migration, and invasion of glioma cells, and it reduced cell apoptosis in glioma cells. It can be concluded that the transcription factor ELF1 may be involved in promoting glioma progression by regulating MEIS1 transcription.

The GFI1 gene, which is a zinc finger transcription factor essential for development of the erythroid and megakaryocytic lineages, was originally discovered in the hematopoietic system, where it functions as a key regulator of stem cell homeostasis, as well as development of the erythroid and megakaryocytic lineages.[22,23] A previous study demonstrated that GFI1 expression is controlled by five distinct regulatory regions spread over 100 kb, with Scl/Tal1 and MEIS1 acting as upstream regulators in early hematopoietic cells.[23] To elucidate the underlying mechanism between GFI1 and MEIS1 in glioma development, MEM analysis was used to reveal that a significant relationship of co-expression between MEIS1 and GFI1 existed. Overexpression of MEIS1 in glioma cells would significantly increase the enrichment of H3K4me1, H3K27ac, and MEIS1 in the GFI1 enhancer region, as well as the promoter region of GFI1, H3K4me3, H3K27ac, and GFI1, suggesting that MEIS1 promoted the expression of GFI1 by activating the enhancer of GFI1. Overexpression of MEIS1 activated the enhancer of GFI1, and then inhibited proliferation and migration and triggered apoptosis in glioma cells. Moreover, recent studies showed that the tumor suppressor FBW7, an E3 ubiquitin ligase that mediates ubiquitination and degradation of oncoproteins,[24] participated in and promoted in the function of MEIS1/GFI1 in glioma cells. MEIS1 could upregulate the activity of the GFI1 enhancer, followed by inhibition of the expression of FBW7 and then promotion of the proliferation, migration, and invasion and suppression of apoptosis of glioma cells.

Finally, a subcutaneous tumor mouse model of U251 cells (interference of ELF1) was established to confirm the anti-tumor effect of

---

enrichment level in the A172 and U251 cells. (G) Western blot analysis of MEIS1 protein expression in A172 and U251 cells. (H) CCK-8 assay of proliferation of A172 and U251 cells upon treatment with si-NC + oe-NC, si-ELF1 + oe-NC, and si-ELF1 + oe-MEIS1. (I) Transwell assay of migration of A172 and U251 cells upon treatment with si-NC + oe-NC, si-ELF1 + oe-NC, and si-ELF1 + oe-MEIS1 (original magnification, ×200). (J) Transwell assay of invasion of A172 and U251 cells upon treatment with si-NC + oe-NC, si-ELF1 + oe-NC, and si-ELF1 + oe-MEIS1 (original magnification, ×200). (K) Annexin V/PI flow cytometry of A172 and U251 cells upon treatment with si-NC + oe-NC, si-ELF1 + oe-NC, and si-ELF1 + oe-MEIS1. (L) Western blot analysis of PCNA, MMP-9, and cleaved capase-3 protein expression in A172 and U251 cells upon treatment with si-NC + oe-NC, si-ELF1 + oe-NC, and si-ELF1 + oe-MEIS1. *$p < 0.05$ compared with input group or si-NC + oe-NC group; #$p < 0.05$ compared with IgG group or si-ELF1+ oe-NC group. The data between two groups were analyzed by an unpaired t test. The data among multiple groups were analyzed by ANOVA with Tukey's post hoc test. Data at different time points among groups were compared by two-way ANOVA, followed by a Bonferroni post-test. The cell experiment was repeated three times.
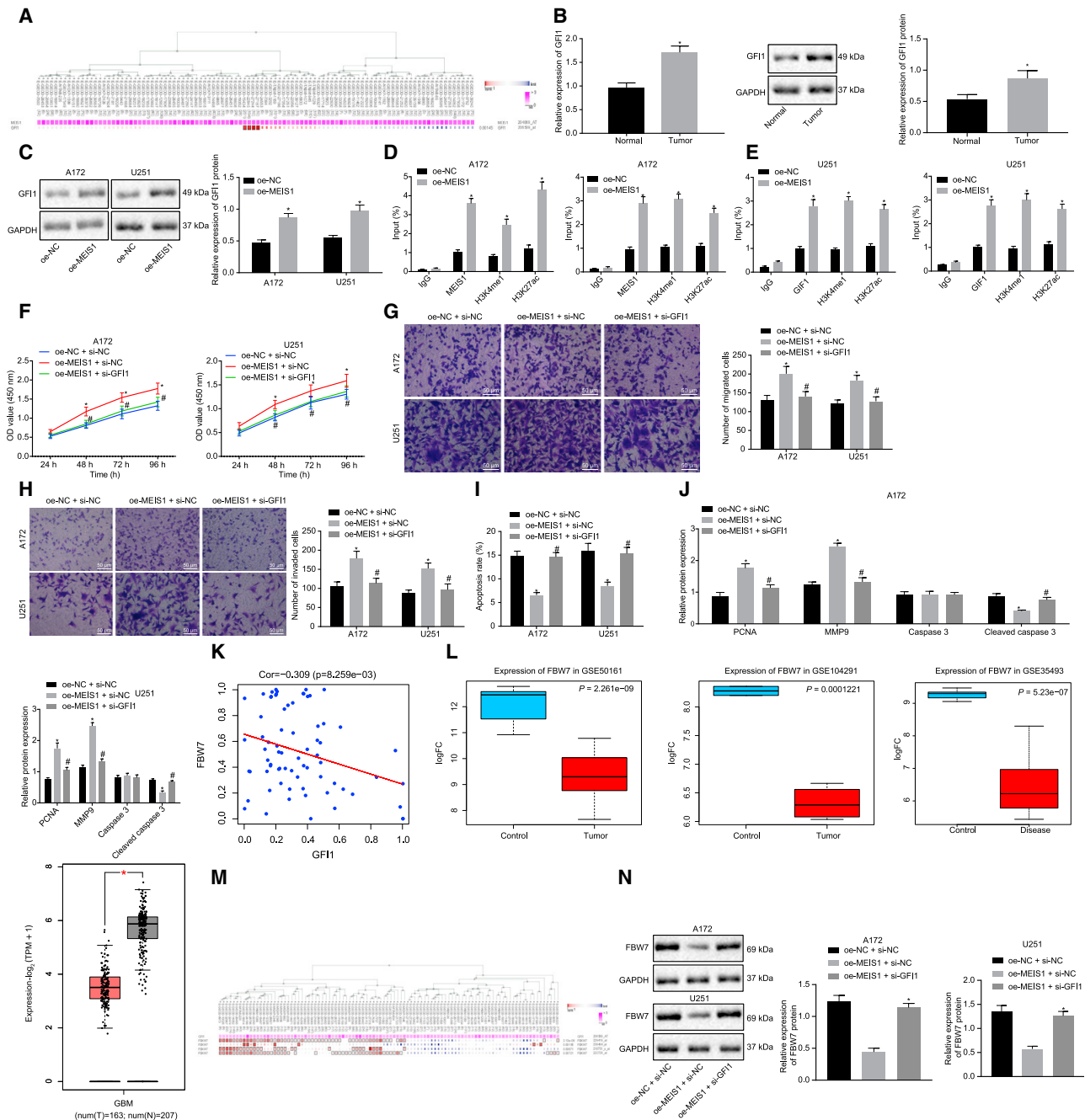
Figure 4. MEIS1 Regulates GFI1 Enhancer Activity in A172 and U251 Glioma Cells

(A) MEM analysis of co-expression relationship between MEIS1 and GFI1. (B) qRT-PCR analysis of GFI1 expression in glioma tissues and normal brain tissues. (C) Western blot analysis of GFI1 expression in A172 and U251 cells upon treatment with oe-NC or oe-MEIS1. (D) ChIP of enrichment of H3K4me1, H3K27ac, and MEIS1 in the GFI1 enhancer region upon treatment with oe-NC or oe-MEIS1. (E) ChIP detected the enrichment of H3K4me1, H3K27ac, and MEIS1 in the promoter region of GFI1 upon treatment with oe-NC or oe-MEIS1. (F) Flow cytometry of A172 and U251 cell proliferation upon treatment with oe-NC + si-NC, oe-MEIS1 + si-NC, or oe-MEIS1 + si-GFI1. (G) Transwell assay of migration of A172 and U251 cells upon treatment with oe-NC + si-NC, oe-MEIS1 + si-NC, or oe-MEIS1 + si-GFI1 (original magnification, ×200). (H) Transwell assay of invasion of A172 and U251 cells upon treatment with oe-NC + si-NC, oe-MEIS1 + si-NC, or oe-MEIS1 + si-GFI1 (original magnification, ×200). (I) Flow cytometry of apoptotic rate of A172 and U251 cells upon treatment with oe-NC + si-NC, oe-MEIS1 + si-NC, or oe-MEIS1 + si-GFI1. (J) Western blot analysis of PCNA, MMP-9 and cleaved capase-3 protein expression in A172 and U251 cells upon treatment with oe-NC + si-NC, oe-MEIS1 + si-NC, or oe-MEIS1 + si-GFI1. (K) Correlation diagram of GFI1 and FBX7 expression through normalization of GEO: GSE50161, GSE104291, and GSE3549 datasets. (L) Boxplot of FBX7 expression from GEO: GSE12657,
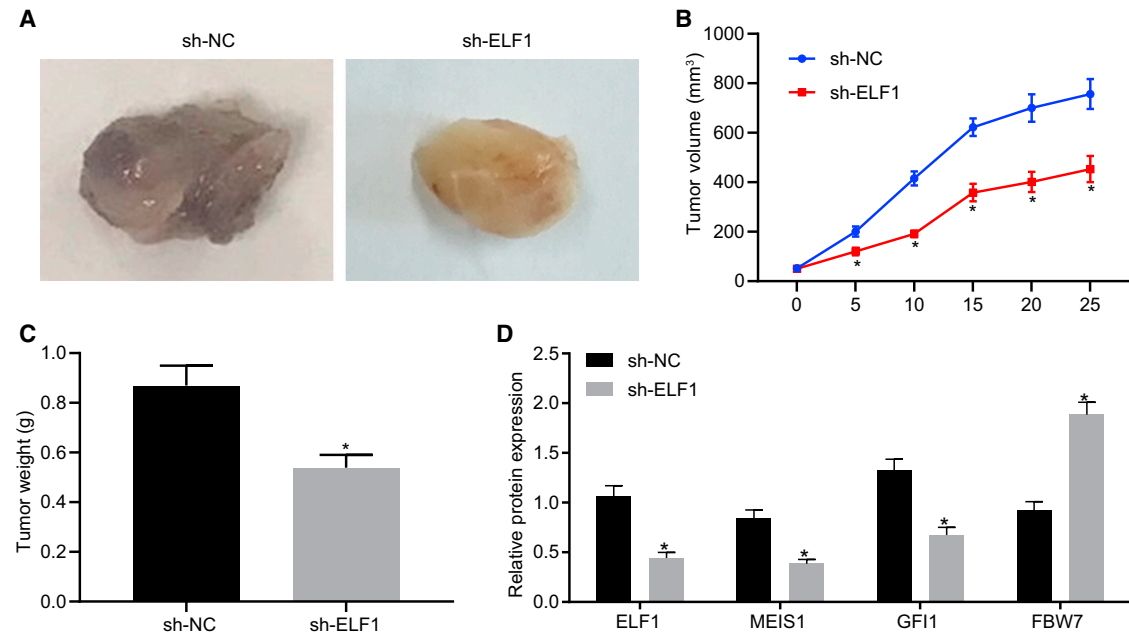
Figure 5. ELF1 Inhibits Tumor Growth in Nude Mice

(A) Representative image of tumor formation upon treatment with sh-NC or sh-ELF1 (n = 5). (B) Statistics of tumor volume growth in nude mice upon treatment with sh-NC or sh-ELF1 (n = 5). (C) Tumor weight statistics of nude mice upon treatment with sh-NC or sh-ELF1 (n = 5). (D) Western blot analysis of ELF1, MEIS1, GFI1, and FBW7 upon treatment with sh-NC or sh-ELF1. *p < 0.05 compared with the sh-NC group. Measurement data are expressed as mean ± standard deviation. The data between two groups were analyzed by an unpaired t test. Data at different time points among groups were compared by two-way ANOVA, followed by a Bonferroni post-test. The cell experiment was repeated three times. n = 5.

ELF1 *in vivo*. The results showed that the growth and weight of tumors in mice treated with si-ELF1 were significantly lower than those in the control group. Additionally, compared with control group, downregulated expressions of ELF1, MEIS1, and GFI1, and upregulated expression of FBW7, were found in tumor tissues treated with si-ELF1. The results showed that interference with ELF1 would inhibit MEIS1/GFI1, thereby promoting expression of FBW7 and retarding glioma growth *in vivo*.

In conclusion, the present study demonstrated that upregulated expression of ELF1 in glioma tissues promoted tumor progression by regulating the MEIS1/GFI1/FBW7 axis (Figure 6), suggesting that ELF1 could serve as a promising therapeutic target for glioma.

MATERIALS AND METHODS

Bioinformatics Analysis

Differential expressed genes were screened using the GEO: GSE12657, GSE35493, GSE104291, and GSE50161 datasets downloaded from the GEO dataset (https://www.ncbi.nlm.nih.gov/gds).

The R language limma package[25] for microarray data was used for differential expression analysis with the threshold set as |log$_2$fold change (FC)| >1 and p value <0.05. The contrasts.fit function of the limma package was used to establish a linear model of the dataset, and eBayes was used to assess the significance of the linear model with a t test and calculate the log$_2$FC value. The expression dataset GEO: GSE12657 contained a total of 12 samples, including 5 normal samples and 7 glioma samples; GEO: GSE35493 contained 7 normal samples and 12 glioma samples; GEO: GSE104291 contained 2 normal samples and 4 glioma samples; and GEO: GSE50161 contained 13 normal samples and 34 glioma samples. Key genes in these expression datasets were obtained by co-expressed analysis through RobustRankAggreg.[26] hTFTarget (http://bioinfo.life.hust.edu.cn/hTFtarget#!/) and Cistrome (http://cistrome.org/) were used to screen human transcription factors. The genes at the intersection of key genes and transcription factors were selected as key transcription factors. The possible downstream regulatory pathways were predicted through the existing literature, and the downstream gene promoter sequence of transcription factor was obtained from the University of California Santa Cruz

GSE35493, GSE50161, and GSE104291 datasets, as well as GBM data from TCGA dataset and GTEx through GEPIA analysis. (M) MEM analysis of co-expression relationship between GFI1 and FBW7. (N) Western blot analysis of FBW7 protein expression in glioma cells upon all treatments. *p < 0.05. Measurement data are expressed as mean ± standard deviation. The data between two groups were analyzed by an unpaired t test. The data among multiple groups were analyzed by ANOVA with Tukey's post hoc test. Data at different time points among groups were compared by two-way ANOVA, followed by a Bonferroni post-test. The cell experiment was repeated three times.
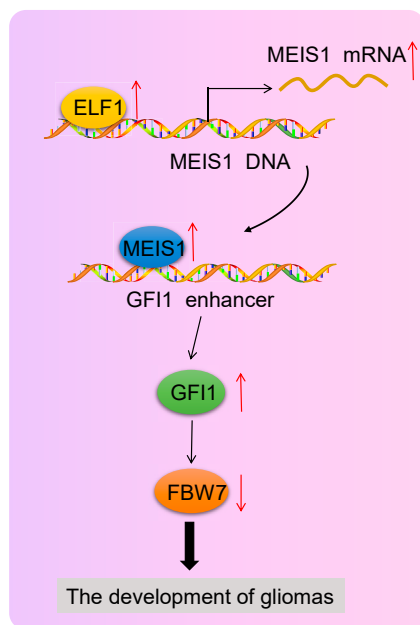
Figure 6. Schematic Map Concerning the Mechanism of ELF1 in Glioma
Upregulated expression of ELF1 in glioma tissues promotes tumor progression by regulating the MEIS1/GFI1/FBW7 axis, suggesting that ELF1 could serve as a promising therapeutic target for glioma.

(UCSC) Genome Browser (http://genome.ucsc.edu/). The binding site of transcription factor and downstream gene was detected through JASPAR (http://jaspar.genereg.net/). We extracted the gene expression data of ELF1, MEIS1, and GFI1 from the normalized data of the GEO: GSE12657, GSE35493, GSE104291, and GSE50161 datasets, followed by Pearson correlation with R language cor.test() function and a t test to assess the significance. The relationship of the downstream pathways was verified by correlation analysis and MEM (https://biit.cs.ut.ee/mem/index.cgi) co-expression analysis. ELF1, MEIS1, and GFI1 expression in glioma was further determined using GBM data of TCGA dataset (https://portal.gdc.cancer.gov/) and normal brain tissue data of the GTEx dataset (https://www.gtexportal.org/home/index.html) with GEPIA (http://gepia2.cancer-pku.cn/#index).

Sample Collection

Sixty glioma specimens confirmed by pathology were collected from 60 patients (male, 38; female, 22; age range, 49–71; average age, 61) underwent surgery from January 2014 to January 2015. According to the 2016 WHO classification of central nervous system tumors,[27] gliomas were classified into four grades and the patients in this study consisted of 29 cases of grade I–II, and 31 cases of grade III–IV, with 35 cases of KPS >70 and 25 cases of KPS <70. Excluded criteria were as follows: patients with other malignant tumor concurrent, incomplete clinical information, serious heart disease, kidney disease, and lung dysfunction. In addition, 24 cases of normal brain tissues removed by internal decompression surgery due to severe craniocerebral injury were taken as the control group. All patients did not accept chemora-

diotherapy before surgery with 5- to 36-month follow-up until January 2020 by telephone or subsequent visit. By the end of follow-up, two patients were lost to follow-up and the follow-up rate was 96.67%. The 3-year overall survival of each patient was observed. All patients in this study signed an informed consent and were approved by our Medical Ethics Committee to comply with the Declaration of Helsinki.

Cell Culture and Transfection

Glioma cell lines A172, U251, and T98G, provided by Stem Cell Bank, Chinese Academy of Sciences, were cultured in RPMI 1640 medium containing 10% fetal bovine serum, 100 U/mL penicillin, and 100 mg/mL streptomycin at 37°C in 5% CO_2.

Cells were transfected according to the experimental requirements. When the cell density reached 90% and was in the logarithmic growth phase, cells were digested with trypsin, made into cell suspension (2.5×10^4 cell/mL), and inoculated on six-well plates (2 mL for each well). Lentiviral vectors were constructed using LV5-GFP (lentiviral gene overexpression vector) and the psih1-h1-copgfp siRNA vector (lentiviral siRNA fluorescence expression vector gene silencing vector). si-ELF1, si-GFI1, oe-MEIS1, and their NCs were all constructed by Thermo Fisher Scientific (Waltham, MA, USA). Lentivirus was packaged in 293T cells, which were cultured in RPMI 1640 complete medium containing 10% fetal bovine serum and passed every other day. When the A172, U251, and T98G cells were in the logarithmic growth phase, they were digested by trypsin and triturated, and 2-mL cell suspensions (1×10^5 cells/mL) were inoculated on six-well plates and cultured overnight at 37°C. Then, the virus (1×10^8 transducing units [TU]/mL) was added to the cells for infection, and cells with stable heredity were obtained and collected for subsequent experiments. The sequence of si-ELF1 was 5′-GGATGTTGCTGAAGAAGAA-3′, and the sequence of si-GIF1 was 5′-CGAGCAGACAGCACTTCAA-3′.

qRT-PCR

Total RNA (Invitrogen, USA) was extracted according to the instructions of TRIzol method, and the RNA was reversely transcribed into cDNA using PrimeScript RT kit (RR037A, Takara, Shiga, Japan) with a system of 10 μL. Then, the reaction liquid was exposed to fluorescence quantitative PCR based on the instructions for the SYBR Premix Ex Taq II kit (RR820A, Takara). The samples were subjected to quantitative real-time PCR using a quantitative real-time PCR system (ABI 7500, Applied Biosystems, Foster City, CA, USA). With GAPDH as an internal control, the $2^{-\Delta\Delta Ct}$ method was used to calculate the relative gene expression. Relevant primers were assigned to Shanghai Sangon Biotech (Shanghai, China) (Table 2).

Protein Extraction and Quantification

About 1×10^6 cells were treated with 1 mL of cell lysate (containing protease inhibitor) (P0013J, Beyotime Biotechnology, Shanghai, China) for 45 min, and then centrifuged for 30 min at 4°C and 8,000 rpm to collect the supernatant. Then, the protein concentration of each sample was determined using a bicinchoninic acid (BCA) kit

Table 2. Primer Sequences Used for qRT-PCR

Targets	Primer Sequence (5′→3′)
ELF1	F: 5′-TGTTGTCCAACAGAACGACCT-3′
	R: 5′-GGAAAAATAGCTGGATCACCA-3′
MEIS1	F: 5′-TCACACTGGCCTTAAAGAGGA-3′
	R: 5′-CCGTAATGGGGTAGATCGTC-3′
GFI1	F: 5′-AGCTGTGTAACACTACCGTGAGGAT-3′
	R: 5′-ACCATGATGAGCTTTGCACACT-3′
GAPDH	F: 5′-GCACCGTCAAGGCTGAGAAC-3′
	R: 5′-TGGTGAAGACGCCAGTGGA-3′

F, forward; R, reverse.

(PC0020, Beijing Solebar Biotechnology, Beijing, China). After electrophoresis, the proteins were transferred to a nitrocellulose membrane (66485, Pall, NY, USA). After membrane transformation, the membrane was blocked in 5% skim milk at room temperature for 2 h, and washed with trimethyl aminomethane buffer brine (in Tris-buffered saline with Tween 20 [TBS/T]) three times, each time for 10 min. The membrane was incubated with the primary antibodies ELF1 (ab64937, 1:500, Abcam, UK), MEIS1 (ab19867, 1:1,000, Abcam), GFI1 (ab21061, 1:1,000, Abcam), MMP-9 (ab38898, 1:1,000, Abcam), PCNA (ab92552, 1:1,000, Abcam), caspase-3 (ab13847, 1:500, Abcam), cleaved caspase-3 (ab32042, 1:500, Abcam), and GAPDH (ab9485, 1:1,000, Abcam). The next day, the membrane was washed at room temperature with TBS/T three times, each time for 5 min. Horseradish peroxidase (HRP)-labeled goat anti-rabbit IgG (ab97051, 1:2,000, Abcam, USA) was added and incubated at room temperature for 1 h. The membrane was washed with TBS/T three times, each for 10 min, immersed in enhanced chemiluminescence (ECL) reaction solution (BM101, Bioimage, USA) for 1 min, and then exposed to X-ray in the dark, and finally the target protein bands were measured. GAPDH was used as internal parameter, and the ratio of gray value of target band and internal reference band was used as the relative expression of protein.

Cell Proliferation Assay

After transfection, A172, U251, and T98G cells were digested and resuspended. The cell concentration was adjusted to 1×10^5 cells/mL, and the cells were inoculated into a 96-well plate with 100 μL/well and routinely cultured overnight. Cells were treated according to the instructions of the CCK-8 kit (Beyotime, Shanghai, China), and cell viability was measured by CCK-8 at 24, 48, 72, and 96 h after inoculation. At each test, 10 μL of CCK-8 detection solution was added, incubated in the incubator for 4 h, and absorbance at 450 nm was tested with an enzyme marker followed the construction of the growth curve.

Cell Invasion Ability Experiment

In the Transwell invasion experiment, the Matrigel stored at −80°C was melted into a liquid overnight at 4°C. Then, 200 μL of Matrigel was added to 200 μL of serum-free medium, after which 50 μL of Matrigel was added to upper chamber and incubated for 2–3 h until the gel became solid. Cells were digested and counted, and the cell suspension was prepared with serum-free medium. Next, 200 μL of cell suspension was added to the upper chamber of each well, and 800 μL of cell suspension was added to the lower chamber containing 20% FBS-conditioned medium. Cells were incubated at 37°C for 20–24 h. After that, a transwell plate was soaked in formaldehyde for 10 min and rinsed with pure water three times. The cells were stained with 0.1% crystal violet at room temperature for 30 min, and the cells on the upper surface were wiped off with cotton balls. Cells on the membrane were observed, imaged, and counted by an inverted microscope. Substrate glue was not required for the transwell migration experiment, and the incubation time was 16 h. Cells from at least four randomly selected microscope regions were counted.

Cell Apoptosis Assay

After transfection for 48 h, the cells were digested with 0.25% trypsin and collected in the flow tube, centrifuged, and the supernatant was discarded. Annexin V-fluorescein isothiocyanate (FITC), PI, and HEPES buffer were incorporated into annexin V-FITC/PI dye at a ratio of 1:2:50 according to the instructions of annexin V-FITC apoptosis assay kit (559763, Becton Dickinson, NY, USA). Then, 1×10^6 cells were resuspended in 100 μL of dye solution, and the cells were oscillated and mixed. After incubation at room temperature for 15 min, 1 mL of HEPES buffer (PB180325, Porcello, Wuhan, China) was added to the solution for oscillating and mixing. FITC and PI fluorescence were detected by excitation of 525-nm and 620-nm bandpass filters at the wavelength of 488 nm to detect cell apoptosis.

ChIP

The EZ-Magna ChIP kit (EMD Millipore) was used for ChIP determination. According to the manufacturer's protocol, the cells were immobilized with 4% paraformaldehyde and incubated with glycine for 10 min to produce DNA-protein cross-linking. The cells were then lysed with a cell lysis buffer and a nuclear lysis buffer and treated with ultrasound to produce 200–300 bp of chromatin fragments (a portion of the DNA as input). Next, lysates were immunoprecipitated by magnetic protein A beads bonded with various antibodies. H3K27ac antibody (ab177178, Abcam) or H3K4me1 (ab176877, Abcam) was added to the target protein group. Negative control was added with rabbit IgG (ab171870, Abcam). Finally, the precipitated DNA was analyzed by qRT-PCR.

In Vivo Animal Experiment

Ten BALB/c male nude mice (age, 4–5 weeks old; weight. 18–22 g) were purchased from Shanghai SLAC Laboratory Animal Co. (Shanghai, China). Lentivirus expressing sh-ELF1 or sh-NC was transfected into the human U251 cell line. Cell suspension (20 μL, 1.0×10^6 cells/mL) was inoculated in nude mice at the abdomen subcutaneously (five mice treated with sh-NC, five with sh-ELF1). Tumors were observed weekly and measured with a Vernier caliper. The formula of for calculating tumor volume (TV) is TV = $\frac{1}{2} \times a \times b^2$, where a is length of tumor and b is width of tumor. Mice

were exposed to euthanasia at 35 days, and tumors of each group were removed, weighed, and imaged. All of the above experimental animals used were approved by the Animal Protection and Use Committee, and all of the animal experiments in this study are in accordance with the management and use principles for local experimental animals.

Immunohistochemistry

Paraffin-embedded tumor tissues were subjected to dewaxing, hydration, xylene I and II dewaxing, and gradient alcohol dehydration. Sections were immersed in 3% H_2O_2 for 10 min, washed with PBS twice for 5 min and repaired with antigen (Beyotime, Shanghai, China) at high pressure for 90 s, and then cooled down at room temperature. Sections were blocked with 5% BSA at 37°C for 30 min and incubated with primary rabbit antibody at 4°C overnight. Then, tissues were incubated with HRP-labeled goat anti-rabbit (ab205718, 1:1,000, Abcam) at 37°C for 30 min. Finally, sections were exposed to Dichlorobenzene (DBA) solution (MXB, Fuzhou, China), stained with hematoxylin for 5 min, and observed by an optical microscope (XSP-36, BSD, Shenzhen, China) and imaged. Five high-power fields were randomly selected from each section, and 200 cells were counted in each field. The number of positive cells <5% was negative, and the number of positive cells ≥5% was positive. The immunohistochemical results were scored by two people independently in a double-blinded fashion.

Statistical Analysis

All of the present data were processed using SPSS21.0 software (IBM, Armonk, NY, USA) and expressed as mean ± standard deviation of three independent experiments. The data between two groups were analyzed by an unpaired t test. The data among multiple groups were analyzed by one-way analysis of variance (ANOVA) with Tukey's post hoc test. Data at different time points among groups were compared by two-way ANOVA or repeated-measures ANOVA. Patient survival was calculated by the Kaplan-Meier method, and the relationship between two indexes was analyzed by Pearson's relation analysis. A log-rank test was used for univariate analysis. $p < 0.05$ was considered statistically significant.

SUPPLEMENTAL INFORMATION

Supplemental Information can be found online at https://doi.org/10.1016/j.omtn.2020.10.015.

ACKNOWLEDGMENTS

We would like to show our sincerest appreciation to the reviewers for their critical comments on this article.

AUTHOR CONTRIBUTIONS

M.C. and Y.Z. designed the study. T.Z., M.X., and Y.W. collated the data and carried out data analyses. M.C. and Z.L. produced the initial draft of the manuscript. All authors have read and approved the final submitted manuscript.

DECLARATION OF INTEREST

The authors declare no competing interests.

REFERENCES

1. Ostrom, Q.T., Gittleman, H., Truitt, G., Boscia, A., Kruchko, C., and Barnholtz-Sloan, J.S. (2018). CBTRUS statistical report: primary brain and other central nervous system tumors diagnosed in the united states in 2011–2015. Neuro-oncol. 20 (Suppl 4), iv1–iv86.

2. Oike, T., Suzuki, Y., Sugawara, K., Shirai, K., Noda, S.E., Tamaki, T., Nagaishi, M., Yokoo, H., Nakazato, Y., and Nakano, T. (2013). Radiotherapy plus concomitant adjuvant temozolomide for glioblastoma: Japanese mono-institutional results. PLoS ONE 8, e78943.

3. Lesueur, P., Lequesne, J., Grellard, J.M., Dugué, A., Coquan, E., Brachet, P.E., Geffrelot, J., Kao, W., Emery, E., Berro, D.H., et al. (2019). Phase I/IIa study of concomitant radiotherapy with olaparib and temozolomide in unresectable or partially resectable glioblastoma: OLA-TMZ-RTE-01 trial protocol. BMC Cancer 19, 198.

4. Chinot, O.L., Wick, W., Mason, W., Henriksson, R., Saran, F., Nishikawa, R., Carpentier, A.F., Hoang-Xuan, K., Kavan, P., Cernea, D., et al. (2014). Bevacizumab plus radiotherapy-temozolomide for newly diagnosed glioblastoma. N. Engl. J. Med. 370, 709–722.

5. Gilbert, M.R., Dignam, J.J., Armstrong, T.S., Wefel, J.S., Blumenthal, D.T., Vogelbaum, M.A., Colman, H., Chakravarti, A., Pugh, S., Won, M., et al. (2014). A randomized trial of bevacizumab for newly diagnosed glioblastoma. N. Engl. J. Med. 370, 699–708.

6. Boxerman, J.L., Zhang, Z., Safriel, Y., Rogg, J.M., Wolf, R.L., Mohan, S., Marques, H., Sorensen, A.G., Gilbert, M.R., and Barboriak, D.P. (2018). Prognostic value of contrast enhancement and FLAIR for survival in newly diagnosed glioblastoma treated with and without bevacizumab: results from ACRIN 6686. Neuro-oncol. 20, 1400–1410.

7. Rogers, T.W., Toor, G., Drummond, K., Love, C., Field, K., Asher, R., Tsui, A., Buckland, M., and Gonzales, M. (2018). The 2016 revision of the WHO Classification of Central Nervous System Tumours: retrospective application to a cohort of diffuse gliomas. J. Neurooncol. 137, 181–189.

8. Brat, D.J., Scheithauer, B.W., Fuller, G.N., and Tihan, T. (2007). Newly codified glial neoplasms of the 2007 WHO Classification of Tumours of the Central Nervous System: angiocentric glioma, pilomyxoid astrocytoma and pituicytoma. Brain Pathol. 17, 319–324.

9. Hovelson, D.H., Udager, A.M., McDaniel, A.S., Grivas, P., Palmbos, P., Tamura, S., Lazo de la Vega, L., Palapattu, G., Veeneman, B., El-Sawy, L., et al. (2018). Targeted DNA and RNA sequencing of paired urothelial and squamous bladder cancers reveals discordant genomic and transcriptomic events and unique therapeutic implications. Eur. Urol. 74, 741–753.

10. Feik, E., Schweifer, N., Baierl, A., Sommergruber, W., Haslinger, C., Hofer, P., Maj-Hes, A., Madersbacher, S., and Gsur, A. (2013). Integrative analysis of prostate cancer aggressiveness. Prostate 73, 1413–1426.

11. Ando, M., Kawazu, M., Ueno, T., Koinuma, D., Ando, K., Koya, J., Kataoka, K., Yasuda, T., Yamaguchi, H., Fukumura, K., et al. (2016). Mutational landscape and antiproliferative functions of ELF transcription factors in human cancer. Cancer Res. 76, 1814–1824.

12. Budka, J.A., Ferris, M.W., Capone, M.J., and Hollenhorst, P.C. (2018). Common ELF1 deletion in prostate cancer bolsters oncogenic ETS function, inhibits senescence and promotes docetaxel resistance. Genes Cancer 9, 198–214.

13. Bhanvadia, R.R., VanOpstall, C., Brechka, H., Barashi, N.S., Gillard, M., McAuley, E.M., Vasquez, J.M., Paner, G., Chan, W.C., Andrade, J., et al. (2018). MEIS1 and MEIS2 expression and prostate cancer progression: a role for HOXB13 binding partners in metastatic disease. Clin. Cancer Res. 24, 3668–3680.

14. Lima, K., Carlos, J.A.E.G., Alves-Paiva, R.M., Vicari, H.P., Souza Santos, F.P., Hamerschlak, N., Costa-Lotufo, L.V., Traina, F., and Machado-Neto, J.A. (2019). Reversine exhibits antineoplastic activity in JAK2^{V617F}-positive myeloproliferative neoplasms. Sci. Rep. 9, 9895.

15. Wang, M., Yang, C., Liu, X., Zheng, J., Xue, Y., Ruan, X., Shen, S., Wang, D., Li, Z., Cai, H., and Liu, Y. (2020). An upstream open reading frame regulates vasculogenic

mimicry of glioma via ZNRD1-AS1/miR-499a-5p/ELF1/EMI1 pathway. J. Cell. Mol. Med. *24*, 6120–6136.

16. Xiang, P., Lo, C., Argiropoulos, B., Lai, C.B., Rouhi, A., Imren, S., Jiang, X., Mager, D., and Humphries, R.K. (2010). Identification of E74-like factor 1 (ELF1) as a transcriptional regulator of the Hox cofactor MEIS1. Exp. Hematol. *38*, 798–808.e2.

17. Cai, H., Zhang, F., and Li, Z. (2018). Gfi-1 promotes proliferation of human cervical carcinoma via targeting of FBW7 ubiquitin ligase expression. Cancer Manag. Res. *10*, 2849–2857.

18. Yao, J.J., Liu, Y., Lacorazza, H.D., Soslow, R.A., Scandura, J.M., Nimer, S.D., and Hedvat, C.V. (2007). Tumor promoting properties of the ETS protein MEF in ovarian cancer. Oncogene *26*, 4032–4037.

19. Madison, B.J., Clark, K.A., Bhachech, N., Hollenhorst, P.C., Graves, B.J., and Currie, S.L. (2018). Electrostatic repulsion causes anticooperative DNA binding between tumor suppressor ETS transcription factors and JUN-FOS at composite DNA sites. J. Biol. Chem. *293*, 18624–18635.

20. Matsuoka, S., Ballif, B.A., Smogorzewska, A., McDonald, E.R., 3rd, Hurov, K.E., Luo, J., Bakalarski, C.E., Zhao, Z., Solimini, N., Lerenthal, Y., et al. (2007). ATM and ATR substrate analysis reveals extensive protein networks responsive to DNA damage. Science *316*, 1160–1166.

21. Mahmoudian, R.A., Bahadori, B., Rad, A., Abbaszadegan, M.R., and Forghanifard, M.M. (2019). *MEIS1* knockdown may promote differentiation of esophageal squamous carcinoma cell line KYSE-30. Mol. Genet. Genomic Med. *7*, e00746.

22. Chowdhury, A.H., Ramroop, J.R., Upadhyay, G., Sengupta, A., Andrzejczyk, A., and Saleque, S. (2013). Differential transcriptional regulation of *meis1* by Gfi1b and its cofactors LSD1 and CoREST. PLoS ONE *8*, e53666.

23. Wilson, N.K., Timms, R.T., Kinston, S.J., Cheng, Y.H., Oram, S.H., Landry, J.R., Mullender, J., Ottersbach, K., and Gottgens, B. (2010). Gfi1 expression is controlled by five distinct regulatory regions spread over 100 kilobases, with Scl/Tal1, Gata2, PU.1, Erg, Meis1, and Runx1 acting as upstream regulators in early hematopoietic cells. Mol. Cell. Biol. *30*, 3853–3863.

24. Cai, J., Sun, M., Hu, B., Windle, B., Ge, X., Li, G., and Sun, Y. (2019). Sorting Nexin 5 controls head and neck squamous cell carcinoma progression by modulating FBW7. J. Cancer *10*, 2942–2952.

25. Ritchie, M.E., Phipson, B., Wu, D., Hu, Y., Law, C.W., Shi, W., and Smyth, G.K. (2015). *limma* powers differential expression analyses for RNA-sequencing and microarray studies. Nucleic Acids Res. *43*, e47.

26. Kolde, R., Laur, S., Adler, P., and Vilo, J. (2012). Robust rank aggregation for gene list integration and meta-analysis. Bioinformatics *28*, 573–580.

27. Louis, D.N., Perry, A., Reifenberger, G., von Deimling, A., Figarella-Branger, D., Cavenee, W.K., Ohgaki, H., Wiestler, O.D., Kleihues, P., and Ellison, D.W. (2016). The 2016 World Health Organization Classification of Tumors of the Central Nervous System: a summary. Acta Neuropathol. *131*, 803–820.